Colloquia: LaThuile15

Measurement of the CP-violating phase γ at LHCb

R. F. Koopman on behalf of the LHCb Collaboration

FOM-Nikhef - Amsterdam, The Netherlands

Summary. — The CKM phase γ is the angle of the unitarity triangle which is least well known. To reach the highest sensitivity to its value, all currently available measurements using hadronic tree decays by LHCb are combined, resulting in $\gamma = (73\,^{+9}_{-10})^\circ$. The combination includes results from measurements of time-integrated CP violation in $B^\pm \to Dh^\pm$ and $B^0 \to DK^{*0}$ decays, with h a pion or kaon, and from a time-dependent measurement of CP violation using $B_s^0 \to D_s^\pm K^\mp$ decays.

PACS `12.15.Hh` – Determination of Cabibbo-Kobayashi & Maskawa (CKM) matrix elements.
PACS `13.25.Hw` – Decays of bottom mesons.

1. – Introduction

In the Standard Model (SM), CP violation is introduced via the Yukawa couplings which describe the interactions of the quarks to the Higgs field. Only the weak interactions violate CP. The flavour changing weak interactions are characterised by the Cabibbo-Kobayashi-Maskawa (CKM) matrix [1],

$$(1) \quad V_{\text{CKM}} = \begin{pmatrix} V_{ud} & V_{us} & V_{ub} \\ V_{cd} & V_{cs} & V_{cb} \\ V_{td} & V_{ts} & V_{tb} \end{pmatrix} \approx \begin{pmatrix} 1 - \frac{1}{2}\lambda^2 & \lambda & A\lambda^3(\rho - i\eta) \\ -\lambda & 1 - \frac{1}{2}\lambda^2 & A\lambda^2 \\ A\lambda^3(1 - \rho - i\eta) & -A\lambda^2 & 1 \end{pmatrix},$$

which is given here in the Wolfenstein parametrisation [2] to $\mathcal{O}(\lambda^4)$. The CKM matrix is a unitary matrix that carries four free parameters, three of which are real parameters and one is a complex phase. It is the imaginary term, $i\eta$, that allows for CP violation in the SM. The relations between the different elements of the CKM matrix can be represented as triangles in the complex plane. The unitarity triangle presented in fig. 1 shows our current knowledge on the CKM matrix. Testing the unitarity of the theory by over-constraining the sides and angles of this triangle provides a direct test of the SM.
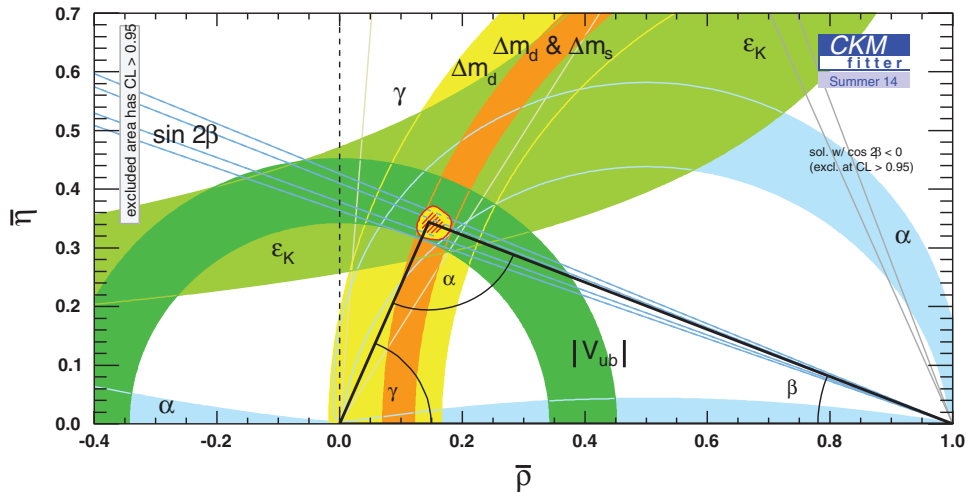
Fig. 1. – Global CKM fit to the unitarity triangle, illustrating our current knowledge on the CKM mechanism [3].

The angle γ is the angle of the unitarity triangle which is least well known. The measurements presented in these proceedings are all performed using hadronic tree decays, which are not sensitive to new physics, and therefore provide a test of the SM. Moreover, they can be used as a benchmark against which measurements sensitive to new physics [4] can be tested. The angle γ is associated to the CKM element V_{ub}, making decays with a $b \to u$ transition sensitive to γ. In order to measure CP violation, one needs to study the interference between two competing decay amplitudes, typically one yielding a $b \to u$ transition and one yielding a $b \to c$ transition. The sensitivity to γ is largest for a large interference, which is achieved when both decay amplitudes are of comparable size.

Different B meson decay channels have been studied resulting in a combined measurement of $\gamma = (73\,^{+9}_{-10})°$ [5]. The different measurements can be divided into two categories: a time-dependent measurement which exploits the decay time structure of B_s^0 decay; and several time-integrated measurements where the event yield of a process and the CP conjugate process are compared.

2. – Selection of events containing B decays

Due to their long lifetime and large boost, B mesons typically fly a few mm before they decay. The excellent vertex resolution of the LHCb detector allows to accurately measure the separation between the primary vertex and the secondary vertex. The B meson decays discussed in these proceedings are all of the type "charmed B meson decays", where the B meson first decays to a "bachelor" hadron and a charm meson with finite lifetime, that then further decays into the final state particles. The type of the various final state particles is determined by the RICH pion/kaon identification. Multivariate analysis, like boosted decision trees, is a commonly used tool to separate the signal from the combinatorial background. Mass fits are used to further separate signal from background, exploiting the outstanding momentum resolution of the LHCb detector.
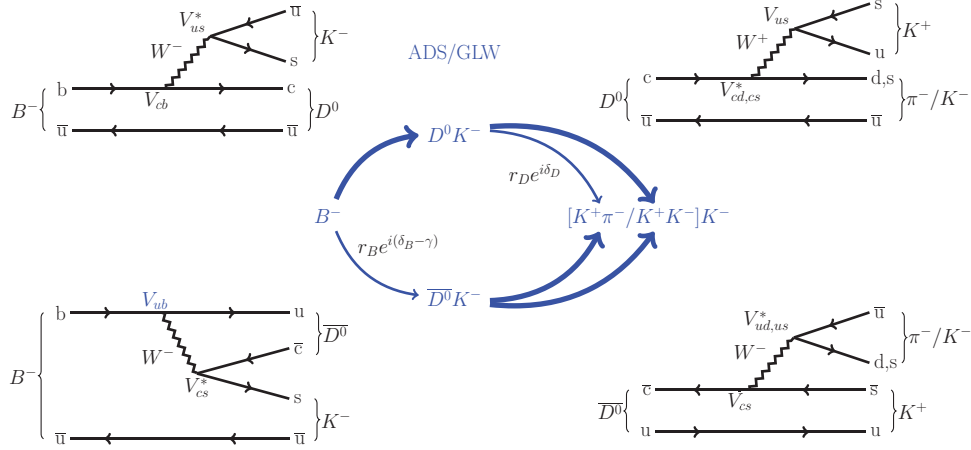
Fig. 2. – Feynman diagrams describing the $B^{\pm} \to Dh^{\pm}$ decay with the subsequent decay of the D meson to a GLW and ADS type final state. The thickness of the arrows indicate the size of the decay amplitude. The parameter r_B (r_D) is the ratio of the suppressed decay amplitude over the favoured amplitude of the B (D) decay, and δ_B (δ_D) the strong phase difference between them.

3. – Direct CP violation in $B^{\pm} \to Dh^{\pm}$ decays

Charged B decays to a neutral D meson and a charged bachelor hadron (pion or kaon) provide a powerful tool for γ determination. The amplitude of $B^{-} \to D^{0}K^{-}$ is proportional to V_{cb}, whereas the amplitude of $B^{-} \to \overline{D}^{0}K^{-}$ is proportional to V_{ub}. The latter is colour suppressed, indicated with the thinner arrow in fig. 2, where r_B is the ratio of the two B decay amplitudes and δ_B and γ are the strong and weak phase difference between them, respectively. Decays with a bachelor kaon are more sensitive to γ than decays with a bachelor pion, due to the larger value of r_B. We choose a D final state which is accessible to both D^0 and $\overline{D}^0$, such that the two amplitudes can interfere. We measure the number of $B^{-} \to DK^{-}$ decays and $B^{+} \to DK^{+}$ decays separately. From these event yields two observables are constructed. A CP asymmetry

$$(2) \qquad A^{DK,f} = \frac{\Gamma(B^{-} \to [D[\to f]K^{-}) - \Gamma(B^{+} \to [D[\to \bar{f}]K^{+})}{\Gamma(B^{-} \to [D[\to f]K^{-}) + \Gamma(B^{+} \to [D[\to \bar{f}]K^{+})},$$

and the charge-averaged ratio of $B^{\pm} \to DK^{\pm}$ to $B^{\pm} \to D\pi^{\pm}$ decays,

$$(3) \qquad R^{f}_{K/\pi} = \frac{\Gamma(B^{-} \to [D[\to f]K^{-}) + \Gamma(B^{+} \to [D[\to \bar{f}]K^{+})}{\Gamma(B^{-} \to [D[\to f]\pi^{-}) + \Gamma(B^{+} \to [D[\to \bar{f}]\pi^{+})}.$$

These observables can be expressed in terms of the weak phase γ, the ratio of decay amplitudes and the strong phase difference [6].

Various D final states satisfy the requirement of accessibility to both the D^0 and the $\overline{D}^0$ meson, presenting interesting opportunities to measure γ at LHCb. The different types of D meson decays are dubbed "GLW" [7, 8], "ADS" [9, 10], "GLS" [11] and "GGSZ" [12], after authors who proposed this type of D meson decays for γ determination.
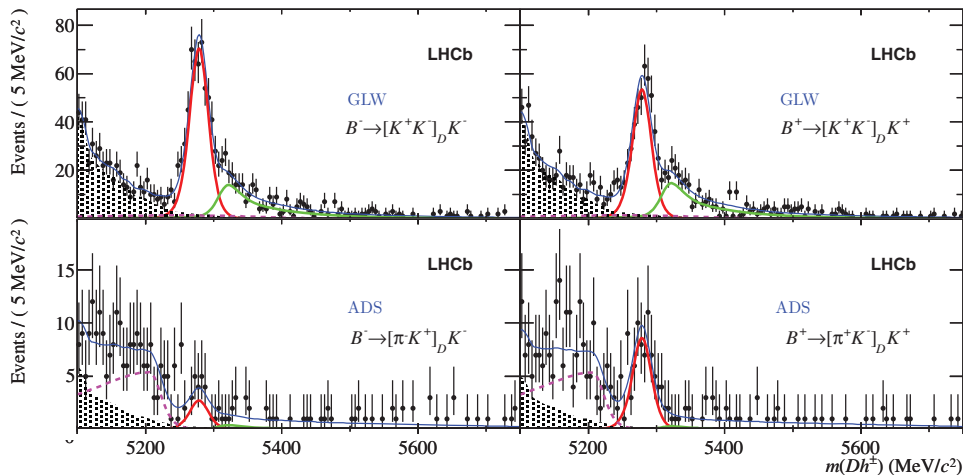
Fig. 3. – Invariant mass distributions of $B^{\mp} \to (K^+K^-)_D K^{\mp}$ and $B^{\mp} \to (\pi^{\mp}K^{\pm})_D K^{\mp}$ decays.

3.1. *GLW and ADS method*. – In the GLW method the D final state is a CP eigenstate. LHCb performed a measurement using the final states K^+K^- and $\pi^+\pi^-$ [13]. For these final states the D^0 and the $\overline{D}^0$ decay amplitudes are equal, as indicated with arrows of the same thickness in fig. 2.

In the ADS method a final state is used which is not a CP eigenstate. LHCb performed a measurement using the D final states $K^{\pm}\pi^{\mp}$ [13] and $K^{\pm}\pi^{\mp}\pi^+\pi^-$ [14]. For these final states one of the D decay amplitudes is doubly Cabibbo-suppressed. In addition to the observables in eqs. (2), (3), the ratio of Cabibbo-suppressed to Cabibbo-favoured decays,

$$(4) \qquad R_{\pm}^{DK,f} = \frac{\Gamma(B^{\pm} \to D[\to f_{\text{sup}}]K^{\pm})}{\Gamma(B^{\pm} \to D[\to f_{\text{fav}}]K^{\pm})},$$

can be extracted and is related to γ.

A large asymmetry, and hence a large sensitivity to γ, is observed for $B^{\pm} \to (K^{\mp}\pi^{\pm})K^{\pm}$ decays, where the favoured $B^- \to D^0K^-$ decay is followed by the doubly Cabibbo-suppressed D^0 decay, while the suppressed $B^- \to \overline{D}^0K^-$ decay is followed by the favoured $\overline{D}^0$ decay. However, the event yields are low compared to the GLW method, where the D^0 decay is singly Cabibbo-suppressed (fig. 3).

3.2. *GLS method*. – Singly Cabibbo-suppressed D decays to final states that are not CP eigenstates provide a valuable information on γ. A large charge asymmetry was found in $D \to K_S^0 K\pi$ decays [15], however, due to the Cabibbo-suppression, the event yields are low, as shown in fig. 4. An additional observable is defined as

$$(5) \qquad R_{fav/sup}^{D\pi} = \frac{\Gamma(B^- \to D[\to f_{\text{fav}}]\pi^-) + \Gamma(B^+ \to D[\to f_{\text{fav}}]\pi^+)}{\Gamma(B^- \to D[\to f_{\text{sup}}]\pi^-) + \Gamma(B^+ \to D[\to f_{\text{sup}}]\pi^+)},$$

and related to γ in ref. [11].

This multibody D decay can proceed through the K^* resonance, and only the phase space around this resonance is used in the analysis to maximise the sensitivity to γ. The
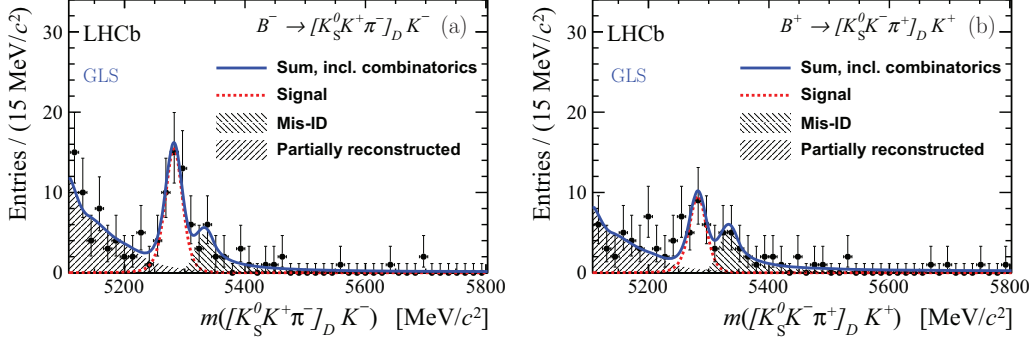
Fig. 4. – Invariant mass distribution of $B^{\mp} \to (K_S^0 K^{\pm} \pi^{\mp})_D K^{\mp}$ decays.

strong phase difference δ_D varies across the Dalitz plot of the D decay due to resonances. The introduction of a coherence factor κ and an average strong phase difference, as first proposed in ref. [16], allows the decay to be treated inclusively, without considering the Dalitz plot positions individually. To avoid a significant modelling uncertainty, the κ and average δ_D measured by CLEO [17] are used.

3'3. *GGSZ method.* – The D final states $K_S^0 \pi^+ \pi^-$ and $K_S^0 K^+ K^-$ [18] are also accessible to both D^0 and $\overline{D}^0$. The asymmetry in the overall yields is expected to be small, however, it can be large in certain areas of the Dalitz plot. This is due to variations in the resonant behaviour across the Dalitz plot, which results in a variation of the strong phase. The D Dalitz plot (fig. 5) is divided into bins, and the event yields of B^- and B^+ decays measured in each bin are used to extract

$$(6) \qquad \begin{aligned} x_{\pm} &= r_B \cos(\delta_B \pm \gamma), \\ y_{\pm} &= r_B \sin(\delta_B \pm \gamma). \end{aligned}$$

This method requires a good understanding of the variation of strong phase in the Dalitz plot, which is measured by CLEO [19].
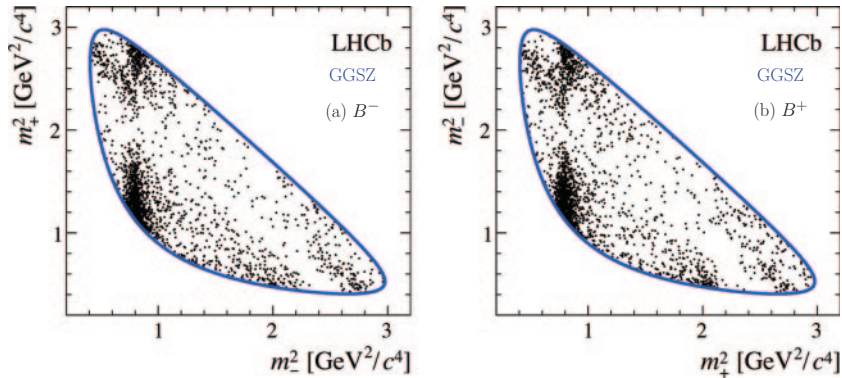

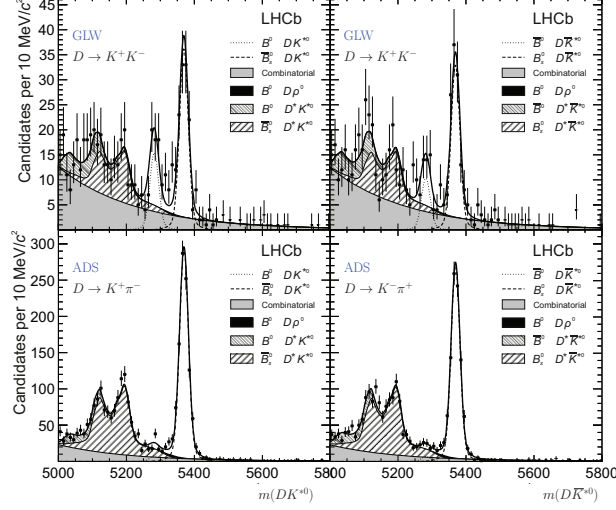Fig. 5. – D Dalitz plot for $B^{\mp} \to (K_S^0 \pi^+ \pi^-)_D K^{\mp}$ decays.

Fig. 6. – Invariant mass distribution for the DK^{*0} and $D\overline{K}^{*0}$ final states, for the GLW mode K^+K^- and the ADS mode $K\pi$. The signal yield for the ADS mode is low as this decay is Cabibbo-suppressed. In addition to the B^0 peak, also the B_s^0 peak is fitted.

4. – Direct CP violation in $B^0 \to DK^{*0}$ decays

In addition to charged B meson decays, neutral B mesons decays add to the sensitivity to γ. In particular, LHCb studied the decay $B^0 \to DK^{*0}$, with the neutral D meson decaying to the GLW modes, K^+K^- and $\pi^+\pi^-$, and the ADS modes, $K^\pm\pi^\mp$ [20]. The observables as defined in eqs. (2)–(4) are measured, from which the angle γ can be extracted.

Interestingly, for neutral B meson decays a large asymmetry is measured for the GLW modes (fig. 6). This can be understood considering the amplitudes of the interfering decay paths. The decays $B^0 \to D^0 K^{*0}$ and $B^0 \to \overline{D}^0 K^{*0}$ are both colour suppressed and therefore similar in size, resulting in a large value of r_B. For the GLW modes, the value of r_D is one. The total decay paths, $B^0 \to DK^{*0}$ following $D \to h^+h^-$, are therefore comparable in size, leading to a large interference for the GLW modes.

5. – Time-dependent analysis of $B_s^0 \to D_s^\pm K^\mp$ decays

CP violation occurs in the decay $B_s^0 \to D_s^\pm K^\mp$ through the interference between mixing and decay [21]. The final states $D_s^+K^-$ and $D_s^-K^+$ are accessible to both the B_s^0 and the $\overline{B}_s^0$ meson. Moreover, the B_s^0 meson can oscillate to a $\overline{B}_s^0$ meson and then decay, or it can decay as B_s^0 meson. The time-dependent decay equations for a initially produced B_s^0 and $\overline{B}_s^0$ decaying to the final state f are given by

$$(7)\ \Gamma_f(t) \simeq e^{-\Gamma_s t}\left[\cosh\left(\frac{\Delta\Gamma_s t}{2}\right) + D_f \sinh\left(\frac{\Delta\Gamma_s t}{2}\right) + C_f \cos(\Delta m_s t) - S_f \sin(\Delta m_s t)\right],$$

$$\Gamma_f(t) \simeq e^{-\Gamma_s t}\left[\cosh\left(\frac{\Delta\Gamma_s t}{2}\right) + D_f \sinh\left(\frac{\Delta\Gamma_s t}{2}\right) - C_f \cos(\Delta m_s t) + S_f \sin(\Delta m_s t)\right],$$
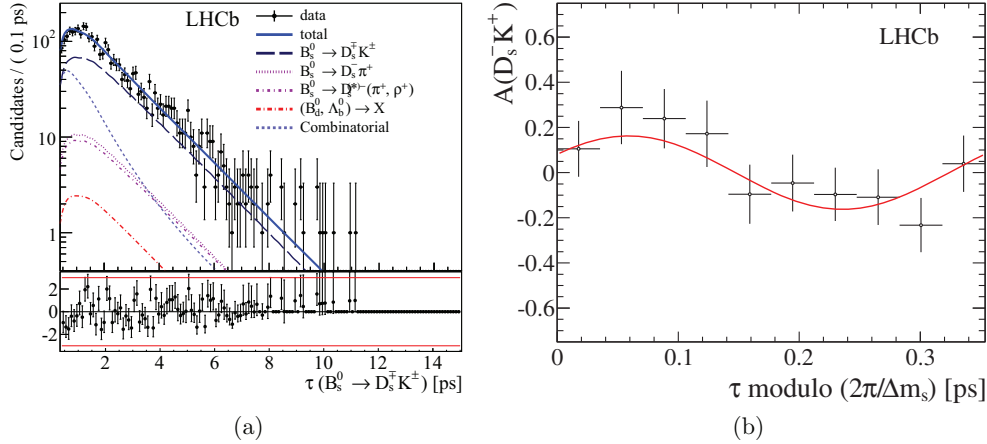
(a) (b)

Fig. 7. – a) Decay time distribution of $B_s^0 \rightarrow D_s^\pm K^\mp$ decays. b) Folded asymmetry using the $D_s^- K^+$ final state.

with Γ_s the average decay width, $\Delta\Gamma_s$ the decay width difference and Δm_s the mass difference between the heavy and light eigenstates. The CP observables D_f, S_f and C_f are related to γ. The CP-conjugate process is described by two additional decay equations which contain three more CP observables, $D_{\bar{f}}$, $S_{\bar{f}}$ and $C_{\bar{f}}$. Under the assumption of no CP violation in either decay or mixing, $C_f = -C_{\bar{f}}$.

After the selection of signal candidates, a multidimensional mass fit is made to extract the yields of the signal and the various sources of background. This fit uses the invariant mass of the B and the D meson and a quantity related to the pion-kaon separation as discriminating variables. The measured yields are used in a subsequent fit to the decay time distribution, from which the CP observables are extracted. The folded asymmetry as a function of folded decay time, measured with the $D_s^- K^+$ final state, are shown in fig. 7.

6. – Combination

The different measurements are combined to give the best precision of γ [5]. The "Robust" combination includes only decays with a kaon bachelor particle. These decays are more sensitive to γ due to the larger value of r_B^K compared to r_B^π. In the "Full" combination, also decays with a pion bachelor particle are included which typically have larger branching fractions but are potentially more affected by the systematic uncertainties.

The combinations follow a frequentist approach. The combined likelihood of all experimental observables is maximised, assuming Gaussian distributions for most observables. In the combination the effects from $D^0 - \overline{D}^0$ mixing are taken into account, as well as effects from CP violation in D^0 decay. The best sensitivity to γ is reached including auxiliary input on the hadronic parameters r_D, δ_D and κ for the different D decays, on CP violation in decay of D decay and on charm mixing. The relevant parameters are measured using data from CLEO [17, 19, 22, 23] and Belle [24] and by HFAG [25]. The angle ϕ_s is constrained to its measured value [26].
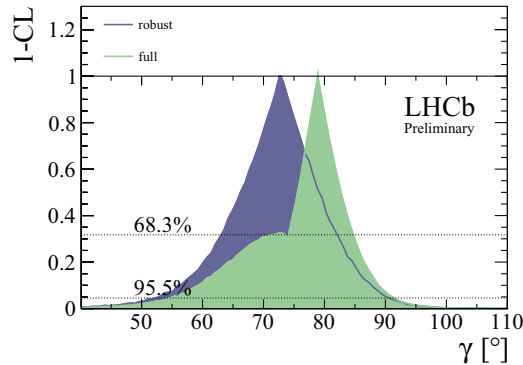
Fig. 8. – 1–CL curves for the Robust and the Full combinations.

The value of γ is found to be $\gamma = (73\,^{+9}_{-10})^\circ$ and $\gamma = (79\,^{+6}_{-7})^\circ$ for the "Robust" and "Full" combination, respectively, and the confidence interval is illustrated in fig. 8. Note that in the "Full" combination, two maxima are found within the 68% confidence level interval: the sharp maximum quoted here and a secondary maximum which coincides with the maxima found in the "Robust" combination. The sharp maximum corresponds to an unexpectedly large value of $r_B^{D\pi}$, which enhances the sensitivity to γ for decays with a bachelor pion.

7. – Conclusion

We reported a measurement of the CKM angle $\gamma = (73\,^{+9}_{-10})^\circ$. This measurement is performed using a combination of different measurements, using the hadronic tree decays $B^\pm \to Dh^\pm$, $B^0 \to DK^{*0}$ and $B_s^0 \to D_s^\pm K^\mp$ which are not sensitive to new physics contributions. LHCb also reported a measurement of the CKM angle γ using $B \to h^+h^-$ decays, which are sensitive to new physics contributions, yielding $\gamma = (63.5\,^{+7.2}_{-6.7})^\circ$ [4]. The two measurements are in agreement within their uncertainty. The measurements are currently statistically limited. The expected sensitivity, 4° and 1° for Run II and the upgrade, respectively, will help to further test the SM.

REFERENCES

[1] KOBAYASHI M. and MASKAWA T., *Prog. Theor. Phys.*, **49** (1973) 652.
[2] WOLFENSTEIN L., *Phys. Rev. Lett.*, **51** (1983) 1945.
[3] CHARLES J. *et al.*, LPT-ORSAY-15-04 (2015).
[4] AAIJ R. *et al.*, *Phys. Lett. B*, **741** (2015) 1.
[5] *Improved constraints on γ: CKM2014 update*, LHCb-CONF-2014-004 (Sep 2014).
[6] AAIJ R. *et al.*, *Phys. Lett. B*, **726** (2013) 151.
[7] GRONAU M. and WYLER D., *Phys. Lett. B*, **265** (1991) 172.
[8] GRONAU M. and LONDON D., *Phys. Lett. B*, **253** (1991) 483.
[9] ATWOOD D., DUNIETZ I. and SONI A., *Phys. Rev. Lett.*, **78** (1997) 3257.
[10] ATWOOD D., DUNIETZ I. and SONI A., *Phys. Rev. D*, **63** (2001) 036005.
[11] GROSSMAN Y., LIGETI Z. and SOFFER A., *Phys. Rev. D*, **67** (2003) 071301.
[12] GIRI A. *et al.*, *Phys. Rev. D*, **68** (2003) 054018.
[13] AAIJ R. *et al.*, *Phys. Lett. B*, **712** (2012) 203.

[14] AAIJ R. *et al.*, *Phys. Lett. B*, **723** (2013) 44.
[15] AAIJ R. *et al.*, *Phys. Lett. B*, **733** (2014) 36.
[16] ATWOOD D. and SONI A., *Phys. Rev. D*, **68** (2003) 033003.
[17] INSLER J. *et al.*, *Phys. Rev. D*, **85** (2012) 092016.
[18] AAIJ R. *et al.*, *JHEP*, **10** (2014) 097.
[19] LIBBY J. *et al.*, *Phys. Rev. D*, **82** (2010) 112006.
[20] AAIJ R. *et al.*, *Phys. Rev. D*, **90** (2014) 112002.
[21] AAIJ R. *et al.*, *JHEP*, **11** (2014) 060.
[22] BONVICINI G. *et al.*, *Phys. Rev. D*, **89** (2014) 072002.
[23] LIBBY J. *et al.*, *Phys. Lett. B*, **731** (2014) 197.
[24] WHITE E. *et al.*, *Phys. Rev. D*, **88** (2013) 051101.
[25] AMHIS Y. *et al.*, FERMILAB-PUB-12-871-PPD (2012) updated results and plots available at `http://www.slac.stanford.edu/xorg/hfag/`.
[26] AAIJ R. *et al.*, *Phys. Rev. D*, **87** (2013) 112010.